



# 1 An integrated hydrological and hydraulic modelling 2 approach for the flood risk assessment over Po river 3 basin.

4 Rita Nogherotto,<sup>1</sup> Adriano Fantini,<sup>1</sup> Francesca Raffaele,<sup>1</sup> Fabio Di  
5 Sante,<sup>1</sup> Francesco Dottori,<sup>2</sup> Erika Coppola,<sup>1</sup> and Filippo Giorgi<sup>1</sup>

6 <sup>1</sup>International Centre for Theoretical Physics, Trieste, Italy

7 <sup>2</sup>European Commission, Joint Research Centre, Ispra, Italy

8

## 9 **Abstract**

10 Identification of flood prone areas is instrumental for a large number of applications, ranging  
11 from engineering to climate change studies, and provides essential information for planning  
12 effective emergency responses. In this work we describe an integrated hydrological and hy-  
13 draulic modeling approach for the assessment of flood-prone areas in Italy and we present  
14 the first results obtained over the Po river (Northern Italy) at a resolution of 90m. River  
15 discharges are obtained through the hydrological model CHyM driven by GRIPHO, a newly-  
16 developed high resolution hourly precipitation dataset. Runoff data is then used to obtain  
17 Synthetic Design Hydrographs (SDHs) for different return periods along the river network.  
18 Flood hydrographs are subsequently processed by a parallelized version of the CA2D hy-  
19 draulic model to calculate the flow over an *ad hoc* re-shaped HydroSHEDS digital elevation  
20 model which includes information about the channel geometry. Modeled hydrographs and  
21 SDHs are compared with those obtained from observed data for a choice of gauging sta-  
22 tions, showing an overall good performance of the CHyM model. The flood hazard maps  
23 for return periods of 50, 100, 500 are validated by comparison with the official flood hazard  
24 maps produced by the River Po Authority (Adbpo) and with the Joint Research Centre's  
25 (JRC) pan-European maps. The results show a good agreement with the available official  
26 national flood maps for high return periods. For lower return periods the results are less  
27 satisfactory but overall the application suggests strong potential of the proposed approach  
28 for future applications.

29

30 **Keywords:** Flood hazard; Flood mapping; CHyM hydrologic model; CA2D hydraulic model.



# 1 Introduction

The last few decades have seen increased interest towards the study of floods, their consequences and the development of measures to reduce their impact. Flood hazard maps are designed to indicate the probability and/or magnitude of inundations over a given area and are used as an important decision making tool for multiple purposes ranging from infrastructure development to disaster response planning. This is also endorsed by the European Union Flood Risk Management Directive (European Commission, 2007), which mandate is the development of flood hazard maps for exposed territories, showing the potential consequences associated with different flood scenarios, in order to guarantee an effective basis for technical, financial and political decisions regarding the flood risk management. Until recently, flood hazard maps were only available for few regions of the globe, and with coarse resolutions, due to the high data and computational requirements of the hydraulic models employed in their production (Moel et al., 2009). The increase of computational power and the availability of remotely sensed datasets, however, have made the application of flood models with higher resolution (less than 1 km) possible even over large domains (Wood et al., 2011).

Different methods to quantify flood hazard can be employed, resulting in different types of flood maps (Moel et al., 2009). Within the different approaches, the common steps are essentially two: 1) the estimation of the discharges for specific return periods and 2) the combination of the discharges with a digital elevation model (DEM) for the creation of the flood map.

For limited area gauged basins, where discharges data are available, the first step can be accomplished by using frequency analyses on discharge records and fitting extreme values distributions (e.g. Te Linde et al., 2008). For larger domains, flood information can be extrapolated to ungauged areas using regionalisation techniques (e.g. Merz and Blöschl, 2005) or by using hydrological models to calculate discharges (Bárdossy, 2007; Khan et al., 2011). These models require spatially explicit meteorological (e.g. temperature, precipitation, evaporation, radiation), soil, and land cover data as input and they solve the water balance for each geographical unit for each time step, to yield the discharges for all river stretches. The strength of this approach is not only the applicability over ungauged regions, but also the possibility of assessing the impact of changes in climate and/or land cover on floods. The second step is usually accomplished by using hydraulic models specifically designed for solving channel and floodplain hydraulic routing. Historically, this was usually performed by modeling fluvial hydraulics with one-dimensional finite difference solutions of the full St. Venant equations (see Fread, 1985; Samuels, 1990), using models such as MIKE11 (Havnø et al., 1995) and HEC-RAS (Brunner, 2002). These schemes describe the river channel and floodplain as a series of cross sections perpendicular to the flow and estimate average velocity and water depth at each cross section. Despite the successful validation of flood inundation extent using low resolution satellite imagery (Bates et al., 1997), the one-dimensional schemes have the drawbacks of being computationally expensive and the areas between the cross sections are not explicitly represented (Samuels, 1990; Bates and De Roo, 2000). Thanks to



the increasing availability of high resolution Digital Elevation Models (DEM) for floodplain areas, two-dimensional distributed models have been developed to allow a better conjunction with the elevation of the channel and of the floodplain surface, and to guarantee the calculation of the water depth and depth-averaged velocity at each computational node at each time step. Examples of such two-dimensional schemes are LISFLOOD-FP (Bates and De Roo, 2000), RBFVM-2D (Zhao et al., 1994) and TELEMAC-2D (Galland et al., 1991). These physically based models solve the Shallow Water Equations (SWEs) and, due to the recent advancement in parallel computing techniques, can be applied over large areas at high resolution. In recent years, a new approach was developed which employs cellular automata (CA) algorithms instead of directly solving the SWEs for each interface: for each timestep, the new state of a cell depends only on the state of the neighbouring cells at the previous timestep, according to a set of rules. This technique allows to model complex physical systems using simple operational rules (Wolfram, 1984), drastically reducing the computational requirements compared to physically based models. These algorithms are therefore well suited for parallel computation and have been successfully used to simulate many types of water related problems (e.g. Coulthard et al., 2007; Krupka et al., 2007; Austin et al., 2013).

An example is the CA2D model developed by Dottori and Todini (2011). The CA2D model uses a 2D cellular automata approach and the equations developed for the LISFLOOD-FP model (Bates et al. (2010)) to make high resolution simulations possible at continental and global scale (Dottori et al. (2016d)).

In this study we describe an integrated hydrological and hydraulic modelling approach which uses the Cetemps Hydrological Model (CHyM, Coppola et al. (2007)) and a modified version of the CA2D hydraulic model, hereinafter referred to as CA2D<sub>par</sub>. CA2D<sub>par</sub> includes a parallel algorithm with the physics of the CA2D model but that can be run with multiple processors to further speed up the computation. Furthermore, to better represent river flow and flooding processes, we produced a re-shaped digital elevation model which includes information about the channel geometry by simulating a "digging" assuming that discharges associated to return periods of 1.5 years produce no floods as they represent the conveyance capacity of the river channel. This model has been used over the entire Italian territory. In the present work we focus on the results obtained over the Po river, which is the river with the largest average daily discharge in the Italian peninsula and in whose basin 40% of the gross domestic product of Italy is produced (Montanari, 2012).

In Section 2 we will describe the observational and modelled data and the method applied for flood hazard assessment of the western basin of the river Po. Section 3 will present the results, by means of a validation of the obtained SDHs, a validation of the hazard maps against observations and against existing flood hazard maps.



## 109 2 Data and methods

110 The approach proposed herein assumes that large scale flood hazard maps can be derived  
 111 from an ensemble of small scale simulations of flood processes, arranged to cover the entire  
 112 river network, as previously demonstrated in literature (Alfieri et al., 2013, 2014; Dottori  
 113 et al., 2016d). The procedure is composed by the following steps: 1) the hydrological sim-  
 114 ulations are setup and calibrated for the production of a long-term discharge time series;  
 115 2) the designed hydrographs are derived for different selected return periods; 3) the flood-  
 116 plain hydraulic simulations are performed and the flood maps for each return period are  
 117 produced. These three different steps will be described in detail in the following subsections.

### 118 2.1 The observational data and the hydrological model CHyM

119 Hydrological simulations are performed using the CETEMPS Hydrological Model (CHyM)  
 120 (Coppola et al., 2007), the distributed hydrological model developed by the CETEMPS  
 121 Center of Excellence at the University of L'Aquila. CHyM uses information from a Digital  
 122 Elevation Model (DEM) and produces a D8 connected river network, using cellular automata  
 123 algorithms to resolve local singularities and no-flow points (Coppola et al., 2007).  
 124 Input precipitation from various sources can be assimilated, including gridded precipitation  
 125 from observations and models. Discharge is routed through each grid cell using continuity  
 126 and momentum equations based on the kinematic shallow water approximation of Lighthill  
 127 and Whitham (1955). CHyM is specifically designed for Italian river catchments and has  
 128 been widely tested for a variety of regions across Italy, and in particular for the Po basin  
 129 (Coppola et al., 2014; Verdecchia et al., 2009; Tomassetti et al., 2005b). For this study,  
 130 nine separate domains are simulated, with a resolution varying between 300 and 900m (Fig.  
 131 1). The domains are matching the operational domains simulated by CETEMPS to forecast  
 132 potential floods using stress indexes (Tomassetti et al., 2005a; Verdecchia et al., 2008), but  
 133 they are higher resolution because the HydroSHEDS Digital Elevation Model is used (Lehner  
 134 et al., 2013), which is specifically conditioned for hydrological usage. The choice of the DEM  
 135 is crucial to ensure correct river routing especially in large, flat areas such as the Po plain.  
 136 The simulations span the period 2001–2016 and are driven by the newly-developed hourly  
 137 precipitation dataset GRIPHO (Fantini et al., 2019; Fantini, 2019), which includes quality-  
 138 controlled data from 3712 precipitation stations covering all of Italy. MM5 weather forecasts  
 139 (Grell et al., 1994), operationally in use at CETEMPS for more than 20 years (see e.g. Bianco  
 140 et al., 2006), are employed to fill data gaps in GRIPHO.  
 141 Further information on the hydrological simulations used for this study, including validation  
 142 against discharge observations, can be found in Fantini (2019, chapters 4 and 5).

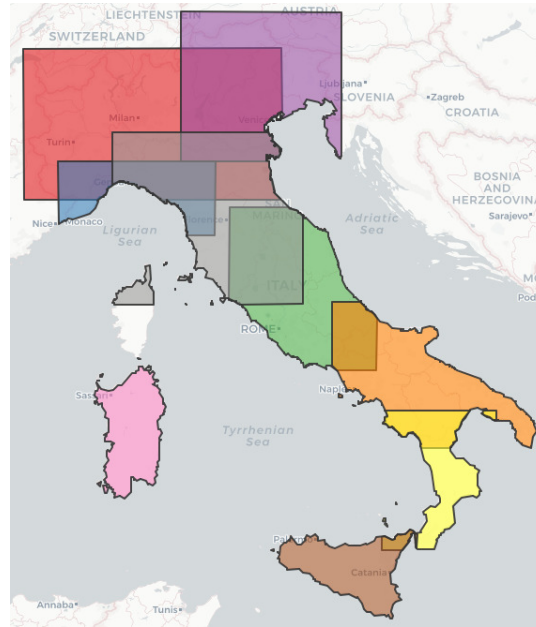


Figure 1: The nine domains on which the CHyM model is run operationally.

## 2.2 Processing the hydrological inputs: the Synthetic Designed Hydrographs (SDHs)

The statistical procedure applied in this study is based on the work of Maione et al. (2003), who performed a Flood Frequency Analysis (FFA) starting from observational data for the Po river basin. The aim is to obtain curves describing the typical discharge timeseries of the event at that river point for the given Return Period. These  $Q_{RP}(t)$  curves will be called Synthetic Design Hydrographs (SDHs) and they represent the discharge ( $Q$ ) of a typical extreme event as a function of the Return Period ( $RP$ ) and the time ( $t$ ). SDHs are estimated and used as input data for the hydraulic model in order to predict the corresponding maximum flood inundation extent and depth (see subsection 2.3). Simulations were performed using observational data described in subsection 2.1 and processed to derive synthetic flood hydrographs throughout a statistical analysis of the Flow Duration Frequency (FDF) reduction curves  $Q_D(RP)$  (Maione et al., 2003). These curves represent the typical discharge with Return Period  $RP$  averaged over any duration  $D$  around the flood peak. For each station along the river network  $Q_D(RP)$  can be calculated from statistical analyses of historical hydrographs. Similarly to the work of Maione et al. (2003) we used the empirical relationship proposed by NERC (1975) defining the reduction ratio ( $\epsilon_D$ ), which is the ratio of the FDF



160 and the peak flood discharge ( $Q_0(RP)$ ), as follows:

$$161 \quad \epsilon_D(RP) = \frac{Q_D(RP)}{Q_0(RP)}. \quad (1)$$

162 In this work we assume  $\epsilon_D$  is independent on the return period, which occurs for medium-large  
163 catchments, as done by Maione et al. (2003) and Alfieri et al. (2013). When performing the  
164 calculation of the FDF around each historical flood peak, the centre of the duration window  
165 of width  $D$  is chosen as to maximise the average computed discharge  $Q_D$ :

$$166 \quad FDF = Q_D = \frac{1}{D} \max \int_t^{t+D} Q(\tau) d\tau, \quad (2)$$

167 where  $t$  and  $\tau$  represent time. The shape of the final synthetic hydrograph will be determined  
168 by the peak-duration ratio  $r_D$  that is the ratio of the time before the peak and the total  
169 duration  $D$  of the averaging window. The smaller the  $r_D$ , the more skewed the hydrograph  
170 will be towards steeper (flatter) rising (falling) limbs of the hydrograph. Centring on  $t = 0$   
171 the peak flood timing, the two limbs of the hydrograph can be described as:

$$172 \quad \int_{-r_D D}^{t=0} Q(\tau) = r_D D Q_D(RP) \quad (3)$$

173 and

$$174 \quad \int_{t=0}^{(1-r_D)D} Q(\tau) = (1 - r_D) D Q_D(RP), \quad (4)$$

175 where  $Q_D(RP)$  is the typical FDF curve for the Return Period  $RP$ . The construction of  
176 the SDH is performed imposing that the maximum discharges for each duration coincides  
177 with the value obtained from the FDF curves, in a given duration  $D$  for each value of the  
178 return period  $RP$ . Thus the SDH is obtained differentiating with respect to the duration  $D$ ,  
179 obtaining for the falling limb:

$$180 \quad SDH = Q_t(RP) = \frac{d/dD[(1 - r_D) D Q_D(RP)]|_{D=D(t)}}{d/dD[(1 - r_D) D]|_{D=D(t)}} \quad (5)$$

181 where  $t = (1 - r_D)D$ .

182 The maximum flood discharge  $Q_0(RP)$  for any given Return Period  $RP$  must then be cal-  
183 culated by fitting an appropriate extreme distribution. Following Alfieri et al. (2015) and  
184 Maione et al. (2003), we chose the Gumbel distribution, so that:

$$185 \quad Q_0(RP) = u - \alpha \ln \left[ -\ln \left( 1 - \frac{1}{RP} \right) \right], \quad (6)$$

186 where the parameters  $u$  and  $\alpha$  are estimated from the fit, and are used for the differentiation  
187 of the equation 5. The equation, representing the falling limb of the SDH, allows us to  
188 calculate a typical flood event discharge timeseries for any location and Return Period,  
189 starting only from the timeseries of yearly maximum discharges. Further details about the  
190 procedure and its implementation can be found in Fantini (2019). Figure 2 shows SDHs for  
191 seven Return Periods obtained applying the procedure described in section 2.2 for a station  
192 on the Tanaro river, a tributary of the Po river.

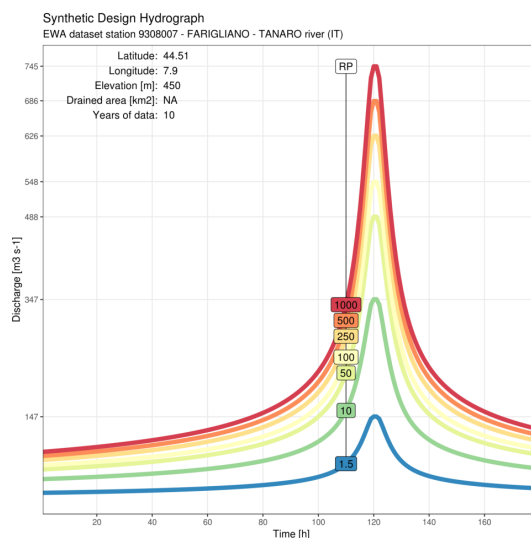


Figure 2: Example Synthetic Design Hydrograph computed following the procedure described in section 2.2 for a station on the Tanaro River, tributary of the Po river. Seven Return Periods (1.5, 10, 50, 100, 250, 500 and 1000 years) are shown.

## 2.3 Modelling the flood inundation: the hydraulic model

Floodplain hydraulic simulations are performed with a modified version of the 2D hydraulic cellular automata model CA2D. The model, described and validated in Dottori and Todini (2011), is based on a simple cell-centred finite volume scheme, which uses the Euler explicit scheme for the integration in time. The momentum equation is solved for each time step, computing volume exchanges between grid cells along the cell's borders. Volumes of each cell are successively updated using volume conservative equations. For this study, the model is run using the semi-inertial formulation of the momentum equation (Bates et al. (2010)), which allows to reproduce channel and floodplain flow processes with a good level of detail with a considerably reduced computational effort (Dottori and Todini, 2011).

The model version CA2D<sub>par</sub> has been written using Fortran90 standard and it has the original model described in Dottori and Todini (2011) as a starting point. The physics is represented on a cartesian 2D grid that allows a good level of scalability. The parallel code has been carried out using the message passing interface (MPI) communications. A number of sub-routines has been introduced in the code to deal with the parallelization and are compiled as separated modules. The parallelization of the code increases as expected the performance of the model which is up to 7.5 times faster respect to the original, even with a limited number of cores (Fig. 3).

The flood inundation extent is dependent on the spatial extent of the performed hydraulic simulations, and it is therefore important to define the number and location of the hydraulic

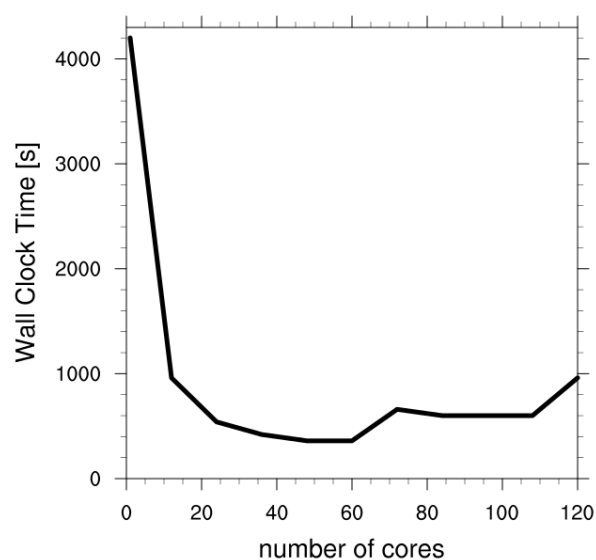


Figure 3: Wall-clock time (s) variation with the number of cores achieved with the parallelization of the CA2D model.





simulation in order to achieve the full coverage of the interested river network. The following section will show the results obtained and it is organised in three steps: 1) calculation of the design flood hydrographs for the available observational stations along the river network using observational data, 2) calculation of the design flood hydrographs obtained using the CHyM model data on the same locations, and comparison of the two series of hydrographs for a validation of the hydraulic model along the Po river, 3) calculation of the design flood hydrographs in selected points along the river network at regular distance from each other and performance of the CA2D<sub>par</sub> simulations using the SDH as inputs.

## 2.4 The production of the flood maps.

Currently the Shuttle Radar Topography Mission (SRTM) digital elevation model (Farr et al., 2007; Rabus et al., 2003) is considered as one of the best openly available data set for flood modeling offering near-global coverage (Hirt et al., 2010; Jing et al., 2014). The void-filled HydroSHEDS variant of SRTM was used in this work with 3 arc sec resolution (Lehner et al., 2006, 2008).

As described in Neal et al. (2012) and Sampson et al. (2015) the inclusion of a river channel network is necessary to guarantee acceptable results in the simulation of flood depths and extent. River widths and depths are however difficult parameters to estimate as it is not possible to measure them remotely on large scales. Natural and artificial river defenses are also challenging to incorporate as their features are smaller than the model grid resolution (Sampson et al., 2015). Moreover their spatial distribution on large scales is not available as literature about fluvial flood defenses generally refers to individual sites (e.g. Brandimarte and Di Baldassarre, 2012; Te Linde et al., 2011). Available remotely sensed data were recently used to generate regional to global estimates of river widths and depths (Andreadis et al., 2013; Gleason and Smith, 2014) by coupling river network data to web based imagery services such as Google maps or Bing maps.

In this study we have used the near-global database of bankfull depths, based on hydraulic geometry equations and the HydroSHEDS hydrography data set described in Andreadis et al. (2013), to estimate the channel conveyance. The idea is to link the channel geometry to the discharge return period, as it guarantees that channels, properly sized, are able to contain the simulated flows and moreover mitigates against the problem of missing information about the river banks. We have used the river bankfull depths information to reshape the HydroSHEDS digital elevation model by assuming a bankfull discharge return period of 1.5 years (Leopold, 1994; Harman et al., 2008; Andreadis et al., 2013; Sampson et al., 2015; Neal et al., 2012). In order to include information about the geometry of the river, the natural and man-made banks, we used the bankfull depths to artificially “dig” the HydroSHEDS DEM until we obtained a no-flood map correspondent to the return period of 1.5 years, which represents the conveyance capacity of the river channel.

As stated in 2.1 a 15-years continuous discharge time series with Italian coverage is generated using the CHyM hydrological model from January 2001 to December 2016. Floodpeaks with 50, 100, 500 year return period are derived for each river point in the model and downscaled



253 to the river network at 3 arc sec resolution. Design flood hydrographs are then used to  
 254 perform small scale floodplain hydraulic simulation on points which will be hereafter referred  
 255 to as “virtual stations” (see Fig. 4), located every 10 km along the river network, for rivers  
 256 with drainage areas larger than  $A=5 \text{ km}^2$ , using the hydraulic model  $CA2D_{par}$ . For each  
 257 virtual station the simulation was run over a sub-domain,  $0.3^\circ \times 0.3^\circ$ , chosen to optimise the  
 258 computational effort, as the simulation time is strongly affected by the size of the domain.  
 259 For each return period a total of 474 simulations were performed and merged to produce a  
 260 Western Po river flood hazard map (Fig. 5).

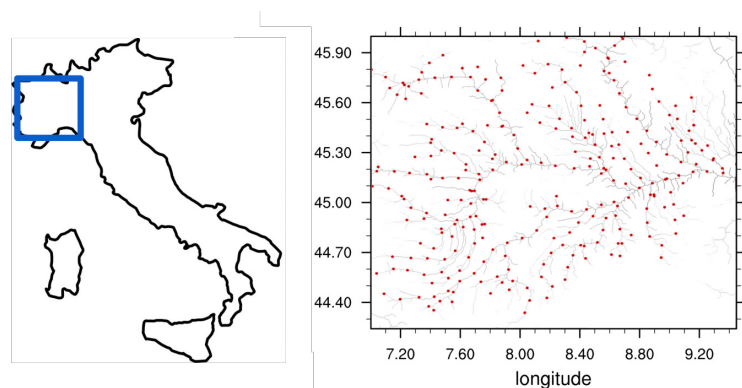


Figure 4: Virtual stations selected for drainage areas larger than  $A=5 \text{ km}^2$  and regularly spaced every 10 km along the high-resolution river network of the analyzed domain (blue box on the left).

## 3 Results

### 3.1 Validation of the SDHs.

264 Tuning and testing of the method were performed on the upper Po basin, due to previous  
 265 experience with the hydrological model on this domain (Coppola et al., 2014), availability of  
 266 reliable observed discharge data, and lack of large water management structures. Due to the  
 267 relatively small size of the simulated domains, the duration of all flood simulations was set  
 268 to 240 h. The SDHs were validated using data from the CHyM model and observations from  
 269 31 gauge stations along the Po river. Figure 6 shows the results of the comparison between  
 270 the SDHs obtained with observational data and those obtained with modelled data. The  
 271 SDHs are generally closely approximated by the model, both in the peaks and in the area  
 272 of the curves. The coefficient of determination ( $R^2$ ) is 0.85 for the SDHs areas and 0.92 for  
 273 the SDHs peaks which are the same values reported in Rojas et al. (2011) for a hydrological  
 274 model of Europe without bias correction of climate data and in Paprotny et al. (2017).

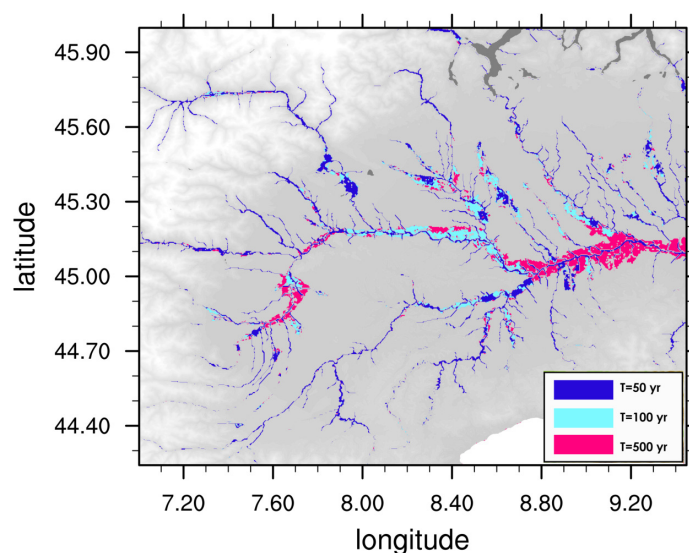


Figure 5: Western Po river flood hazard map for the Return Periods of 500, 100 and 50 years.

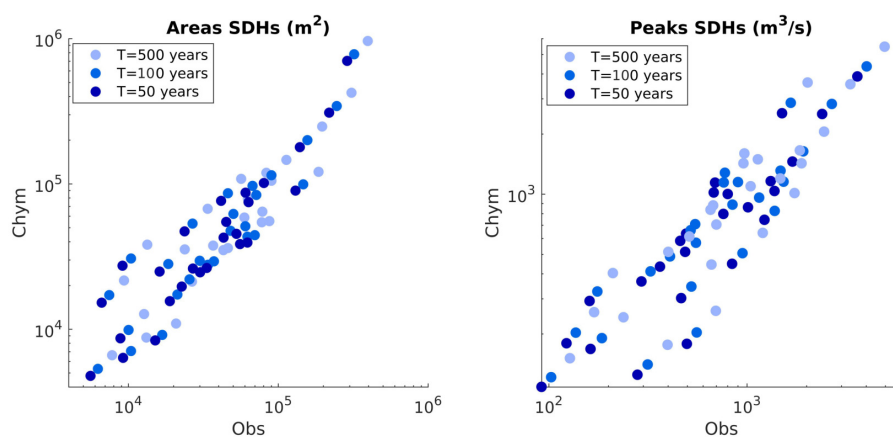


Figure 6: Comparison of simulated (CHyM) and observed (Obs) SDHs areas (a) and discharges peaks (b) for 31 gauge stations along the Po river, for three return periods.



### 3.2 Comparison against observations: a case study

Validation of flood hazard models is achieved through the evaluation of the model accuracy in estimating the probability of flood occurrence and the evaluation of relevant hazard variables of an event (e.g. flood extent and depth, flow velocity). Unfortunately the evaluation is strongly limited by the scarce availability of reference flood maps and flood observations and is a key topic in flood risk analysis. Various methods were suggested by previous studies. One consists in comparing the produced maps with previous maps based on statistical estimation of peak discharges (Pappenberger et al., 2012); another method performs a qualitative assessment of the flood events against satellite flood images (Rudari et al., 2015).

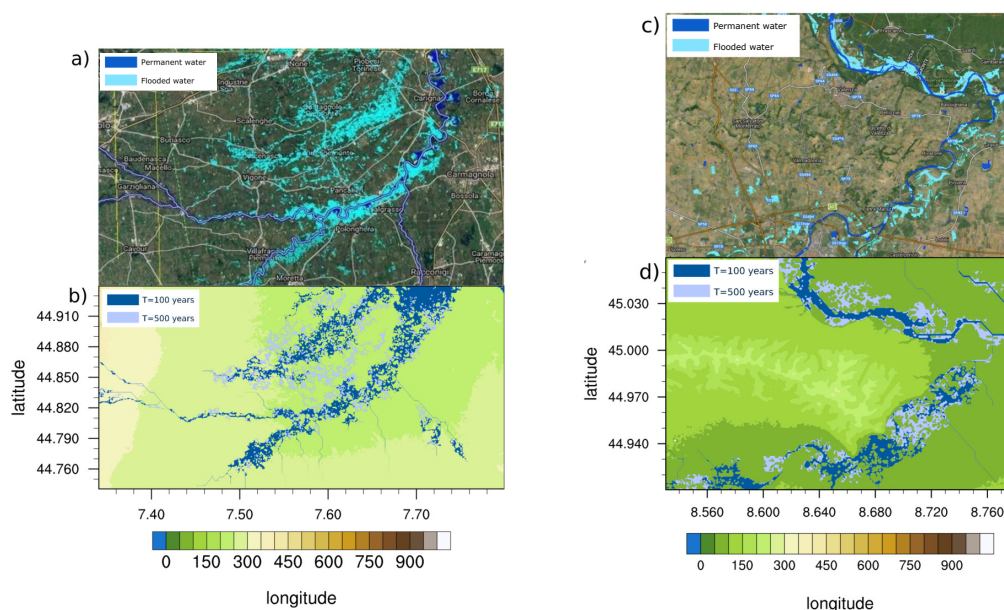


Figure 7: Case studies in November 2016, used for the validation of the method: panels above show floods as acquired by the satellite COSMO-SkyMed (COSMO-SkyMed Image ©ASI (2016). All rights reserved). Panels below show floods as modelled by the integrated CHyM-CA2D<sub>par</sub> method. Panels (a) and (b) show flooded areas in the south of Turin. Panels (c) and (d) show flooded areas in the area of Alessandria.

In order to perform a first validation of the flood hazard mapping methodology we consider a case study of a flood recently occurred in Northern Italy, catalogued as an event with return period of 100 years. November 2016 was characterized by a heavy rainfall event involving the territory of North West of Italy, in particular the Regions of Piemonte and Liguria. The bad



289 weather conditions and the persistence of precipitations caused the increase of hydrometric  
 290 levels of all the rivers in particular in the Po river basin.

291 Figures 7 (a) and (c) show the images from satellite COSMO-SkyMed (CSK) (Covello et al.,  
 292 2010), a four-satellite constellation which gives the possibility of acquiring X -band Syn-  
 293 thetic Aperture Radar (SAR) data day and night, regardless of weather conditions and is  
 294 fully operational since the 2008. It provides radar data characterized by short revisit time  
 295 and therefore useful for flood mapping evaluation. The lower panels show the flood maps  
 296 corresponding to two different return periods ( $T=500$  and  $T=100$  years). We can see that  
 297 the observed event, associated to a return period of 100 years, is fairly good represented by  
 298 the model (Fig. 7 (b) and (d)) as the maps include the particular events observed.

### 299 3.3 Comparison against existing flood hazard maps

300 Another approach for the validation is to perform an evaluation against existing high-  
 301 resolution flood hazard maps (Alfieri et al., 2013; Sampson et al., 2015; Winsemius et al.,  
 302 2016). The evaluation of simulated flood maps against reference maps is performed using  
 303 the indexes proposed in literature (Dottori et al., 2016d; Bates and De Roo, 2000; Alfieri  
 304 et al., 2014). The Hit Ratio index (HR), defined as:

$$305 \quad HR = (F_m \cap F_o) / (F_o) \quad (7)$$

306 evaluates the agreement of modelled maps ( $F_m$ ) with existing maps ( $F_o$ ). This index does  
 307 not take into account the overprediction and underprediction of the flooded area, therefore  
 308 two other measures are calculated to account for this: the False Alarm index (FA), defined  
 309 as

$$310 \quad FA = [F_m - (F_m \cap F_o)] / (F_o) \quad (8)$$

311 where  $F_m - (F_m \cap F_o)$  is the flooded area wrongly predicted by the model, and the Critical  
 312 Success index (CS), defined as:

$$313 \quad CS = (F_m \cap F_o) / (F_m \cup F_o). \quad (9)$$

314 The produced flood hazard maps, hereinafter referred to as “CA2D maps”, are tested against  
 315 the official hazard AdbPo flood maps (<http://www.adbpo.gov.it>), produced by the River Po  
 316 Authority, who classifies the flood plain of the Po river into three levels corresponding to  
 317 return periods of 20-50 years (high frequency), 100-200 years (medium frequency) and 500  
 318 years (low frequency).

319 In addition, we compare the CA2D maps with the flood hazard maps produced by the Joint  
 320 Research Centre of the European Commission (JRC). The JRC maps are freely available on-  
 321 line and are based on streamflow data from the European Flood Awareness System (EFAS  
 322 (Demeritt et al., 2013) and also calculated with a spatial resolution of 3” (Dottori et al.,  
 323 2016a,b,c). To perform the indexes calculations, we have focused our analysis on a smaller

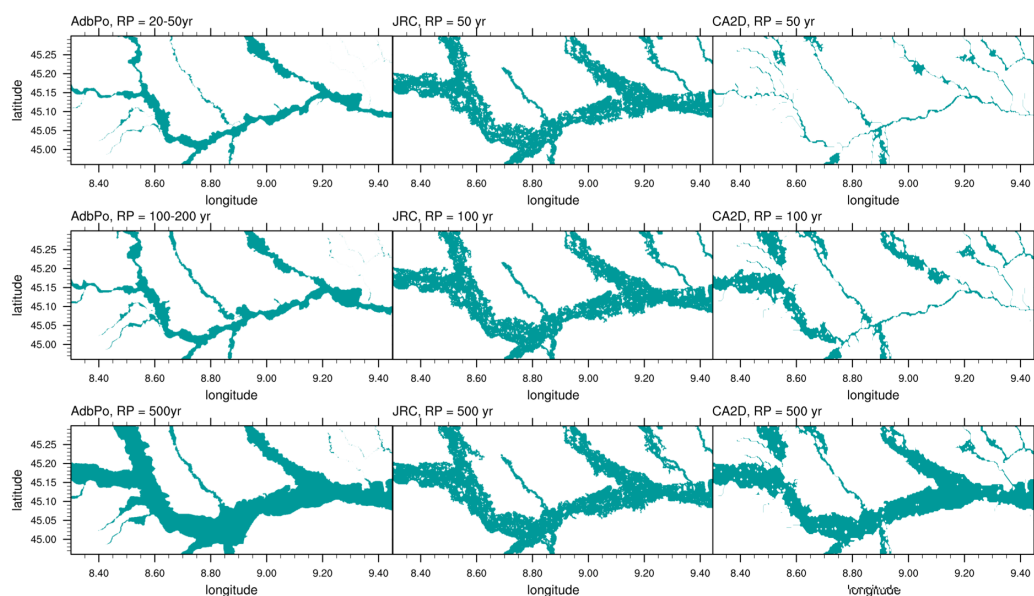


Figure 8: Adbpo, JRC and CA2D flood hazard maps for the 50 years return period (upper panels), 100 years return period (central panels) and 500 years return period (lower panels)





portion of the domain, centred on the main river, removing flooded areas originating from river sections with an upstream area smaller than 500 km<sup>2</sup> since they are not simulated and therefore not included in the JRC maps. The JRC flood maps used for the comparison do not consider flood defences and river geometry, for this reason we only calculate the performance indices (Eq. (7), (8) and (9)) for the 500 years return period, reported in Table 1. Indices are calculated for the CA2D and JRC maps ( $F_m$ ) against the Adbpo maps ( $F_o$ ).

	Hit Rate	False Alarm	Critical Success
JRC	0.83	0.15	0.73
CA2D	0.76	0.12	0.67

Table 1: Evaluation of the CA2D and JRC flooded extent against official flood hazard maps (Adbpo) for three return period of 500 years.

As can be seen, the CA2D maps provide fairly good results for the 500 years return period, with a HR of 0.76, a CS index of 0.67 and a very low false alarm value (0.12), while results are less satisfactory for lower return periods, with considerable underestimation of flood extent respect to the official maps (see Fig. 8). JRC maps also show fair results for the 500 years return period, with a HR of 0.83, a CS of 0.73 and FA of 0.15, and are similar to CA2D maps (Fig. 9), but they systematically overestimate flood extent for the lower return periods (see Fig. 8). The differences between modelled and official maps are partly due to the topography of the Po floodplain, which is not reproduced in the STRT used by both JRC and CA2D maps. Indeed, the area enclosed by the main levees has a complex system of minor embankments, which are designed for lower flood return periods than the main levees (Castellarin et al., 2011). This explains why AdbPo maps are quite similar for return periods of 20-50 years and 100-200 years (see Figure 8).

The narrow extent of flooded areas for return periods of 50 and 100 years in sectors of the river network suggests that the channel conveyance may be overestimated in CA2D maps. However also our reference AdbPo maps show very similar flood extents for return periods of 20-50 and 100-200 years as explained above, therefore the CA2D underestimation can not be quantified. Future work will anyway refine the methodology of channel "digging". This is indeed an open research question, due to the absence of large-scale methods or datasets to estimate river channel depth (Dottori et al., 2016d). Nevertheless, it is worth noting that the method presented here improves the sensitivity to return period of flood extent maps. Conversely, JRC maps calculated for different return period have limited differences, due to the absence of river geometry details. These results confirm that the inclusion of a river channel network is necessary to guarantee acceptable results in the simulation of flood depths and extent for all return periods (Neal et al., 2012).

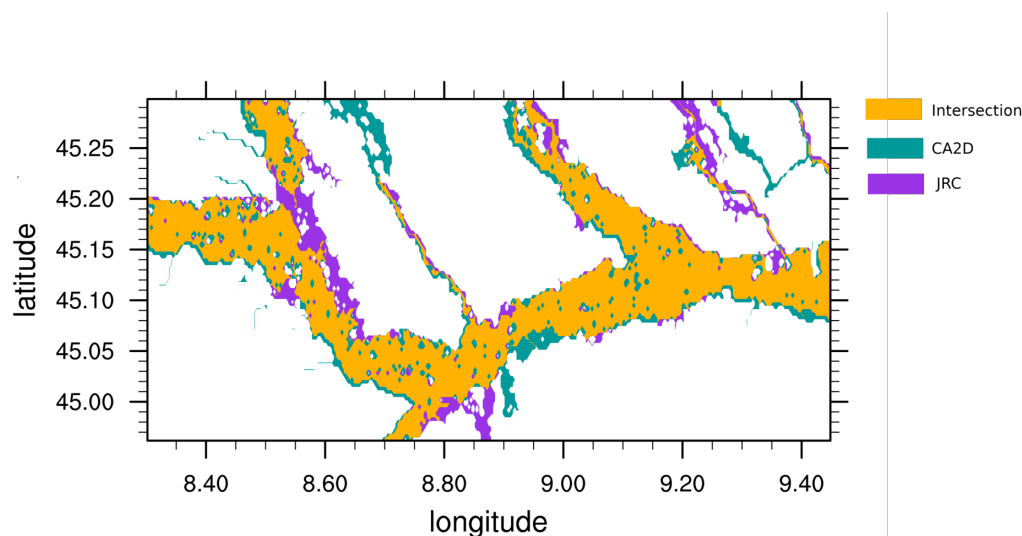


Figure 9: CA2D and JRC flood hazard maps for the 500 years return period

## 4 Conclusions

In this paper we investigate the feasibility of producing high-resolution flood maps using an innovative approach which reshapes the digital elevation models by simulating a "digging" assuming that no floods take place for discharges associated to the return period of 1.5 years, representing the conveyance capacity of the river channel. The main purpose of this method development is to be able to apply it also in those regions where there are no available information about river natural and man-made banks. A 2-dimensional hydraulic model is used to simulate the propagation of the hydrographs across the HydroSHEDS void filled DEM, which was processed to yield an estimate of bankfull discharge. The evaluation of the produced flood maps was performed through some case studies of observed flood extent satellite data, and through existing flood maps over the entire domain, showing a good spatial agreement with observations for high return periods. Comparison for lower return periods showed that the DEM-reshaping method improves the sensitivity to return period of flood extent maps but needs further improvement, for instance, combining observed data about river bed depth and width and discharge (Yamazaki et al., 2014). The validation of the method in a region where all the hydrological and hydraulic information are available will allow us to extend the method elsewhere.





## 5 Acknowledgments

The authors gratefully acknowledge the financial support of the Allianz Insurance Company for the realization of this project.

## References

- Alfieri, L., Burek, P., Dutra, E., Krzeminski, B., Muraro, D., Thielen, J., and Pappenberger, F.: GloFAS-global ensemble streamflow forecasting and flood early warning, *Hydrology and Earth System Sciences*, 17, 1161, 2013.
- Alfieri, L., Salamon, P., Bianchi, A., Neal, J., Bates, P., and Feyen, L.: Advances in pan-European flood hazard mapping, *Hydrological processes*, 28, 4067–4077, 2014.
- Alfieri, L., Burek, P., Feyen, L., and Forzieri, G.: Global warming increases the frequency of river floods in Europe, *Hydrology and Earth System Sciences*, 19, 2247–2260, 2015.
- Andreadis, K., Schumann, G., and Pavelsky, T.: A simple global river bankfull width and depth database, *Water Resources Research*, 49, 7164–7168, 2013.
- Austin, R., Chen, A., Savic, D., and Djordjevic, S.: Fast Simulation of Sewer Flow using Cellular Automata, *NOVATECH 2013*, 2013.
- Bárdossy, A.: Calibration of hydrological model parameters for ungauged catchments, *Hydrology and Earth System Sciences Discussions*, 11, 703–710, 2007.
- Bates, P. and De Roo, A.: A simple raster-based model for flood inundation simulation, *Journal of Hydrology*, 236, 54–77, 2000.
- Bates, P., Horritt, M., Smith, C., and Mason, D.: Integrating remote sensing observations of flood hydrology and hydraulic modelling, *Hydrological Processes*, 11, 1777–1795, 1997.
- Bates, P., Horritt, M., and Fewtrell, T.: A simple inertial formulation of the shallow water equations for efficient two-dimensional flood inundation modelling., *Journal of Hydrology*, 387, 33–45, 2010.
- Bianco, L., Tomassetti, B., Coppola, E., Fracassi, A., Verdecchia, M., and Visconti, G.: Thermally driven circulation in a region of complex topography: Comparison of wind-profiling radar measurements and MM5 numerical predictions, *Annales Geophysicae*, doi: 10.5194/angeo-24-1537-2006, 2006.
- Brandimarte, L. and Di Baldassarre, G.: Uncertainty in design flood profiles derived by hydraulic modelling, *Hydrology Research*, 43, 753–761, 2012.



- 403 Brunner, G.: Hec-ras (river analysis system), in: North American Water and Environment  
 404 Congress & Destructive Water, pp. 3782–3787, ASCE, 2002.
- 405 Castellarin, A., Di Baldassarre, G., and Brath, A.: Floodplain management strategies for  
 406 flood attenuation in the river Po, *River Research and Applications*, 27, 1037–1047, 2011.
- 407 Coppola, E., Tomassetti, B., Mariotti, L., Verdecchia, M., and Visconti, G.: Cellular au-  
 408 tomata algorithms for drainage network extraction and rainfall data assimilation, *Hydro-*  
 409 *logical Sciences Journal*, 52, 579–592, 2007.
- 410 Coppola, E., Verdecchia, M., Giorgi, F., Colaiuda, V., Tomassetti, B., and Lombardi, A.:  
 411 Changing hydrological conditions in the Po basin under global warming, *Science of the*  
 412 *Total Environment*, 493, 1183–1196, 2014.
- 413 Coulthard, T., Hicks, D., and Van De Wiel, M.: Cellular modelling of river catchments and  
 414 reaches: advantages, limitations and prospects, *Geomorphology*, 90, 192–207, 2007.
- 415 Covello, F., Battazza, F., Coletta, A., Lopinto, E., Fiorentino, C., Pietranera, L., Valentini,  
 416 G., and Zoffoli, S.: COSMO-SkyMed an existing opportunity for observing the Earth,  
 417 *Journal of Geodynamics*, 49, 171–180, 2010.
- 418 Demeritt, D., Nobert, S., Cloke, H. L., and Pappenberger, F.: The European Flood Alert  
 419 System and the communication, perception, and use of ensemble predictions for opera-  
 420 tional flood risk management, *Hydrological Processes*, 27, 147–157, 2013.
- 421 Dottori, F. and Todini, E.: Developments of a flood inundation model based on the cellular  
 422 automata approach: testing different methods to improve model performance, *Physics and*  
 423 *Chemistry of the Earth, Parts A/B/C*, 36, 266–280, 2011.
- 424 Dottori, F., Alfieri, L., Salamon, P., Bianchi, A., Feyen, L., and Lorini, V.: Flood hazard  
 425 map for Europe, 100-year return period, European Commission, Joint Research Cen-  
 426 tre (JRC)[Dataset] PID: [http://data.europa.eu/89h/jrc-floods-floodmap.eu\\_rp100y-tif](http://data.europa.eu/89h/jrc-floods-floodmap.eu_rp100y-tif),  
 427 2016a.
- 428 Dottori, F., Alfieri, L., Salamon, P., Bianchi, A., Feyen, L., and Lorini, V.: Flood hazard  
 429 map for Europe, 50-year return period, European Commission, Joint Research Centre  
 430 (JRC)[Dataset] PID: [http://data.europa.eu/89h/jrc-floods-floodmap.eu\\_rp50y-tif](http://data.europa.eu/89h/jrc-floods-floodmap.eu_rp50y-tif), 2016b.
- 431 Dottori, F., Alfieri, L., Salamon, P., Bianchi, A., Feyen, L., and Lorini, V.: Flood hazard  
 432 map for Europe, 500-year return period, European Commission, Joint Research Cen-  
 433 tre (JRC)[Dataset] PID: [http://data.europa.eu/89h/jrc-floods-floodmap.eu\\_rp500y-tif](http://data.europa.eu/89h/jrc-floods-floodmap.eu_rp500y-tif),  
 434 2016c.
- 435 Dottori, F., Salamon, P., Bianchi, A., Alfieri, L., Hirpa, F., and Feyen, L.: Development and  
 436 evaluation of a framework for global flood hazard mapping, *Advances in water resources*,  
 437 94, 87–102, 2016d.
- 438 European Commission: Directive 2007/60/EC of the European Parliament and of the Coun-



- 439 cil of 23 October 2007 on the assessment and management of flood risks, J. Eur. Union,  
 440 L 288, 27–34, 2007.
- 441 Fantini, A.: Climate change impact on flood hazard over Italy, Ph.D. thesis, University of  
 442 Trieste, 2019.
- 443 Fantini, A., Coppola, E., Verdecchia, M., and Giuliani, G.: GRIPHO : a gridded high-  
 444 resolution hourly precipitation dataset over Italy, in preparation, 2019.
- 445 Farr, T., Rosen, P., Caro, E., Crippen, R., Duren, R., Hensley, S., Kobrick, M., Paller,  
 446 M., Rodriguez, E., Roth, L., et al.: The shuttle radar topography mission, *Reviews of*  
 447 *geophysics*, 45, 2007.
- 448 Fread, D.: Channel routing, *Hydrological forecasting*, pp. 437–503, 1985.
- 449 Galland, J.-C., Goutal, N., and Hervouet, J.-M.: TELEMAC: A new numerical model for  
 450 solving shallow water equations, *Advances in Water Resources*, 14, 138–148, 1991.
- 451 Gleason, C. and Smith, L.: Toward global mapping of river discharge using satellite im-  
 452 ages and at-many-stations hydraulic geometry, *Proceedings of the National Academy of*  
 453 *Sciences*, 111, 4788–4791, 2014.
- 454 Grell, G., Dudhia, J., and Stauffer, D.: A description of the fifth-generation Penn  
 455 State/NCAR Mesoscale Model (MM5), Tech. Rep. December, doi:10.5065/D60Z716B,  
 456 1994.
- 457 Harman, C., Stewardson, M., and DeRose, R.: Variability and uncertainty in reach bankfull  
 458 hydraulic geometry, *Journal of hydrology*, 351, 13–25, 2008.
- 459 Havnø, K., Madsen, M., and Dørge, J.: MIKE 11—a generalized river modelling package,  
 460 *Computer models of watershed hydrology*, pp. 733–782, 1995.
- 461 Hirt, C., Filmer, M., and Featherstone, W.: Comparison and validation of the recent freely  
 462 available ASTER-GDEM ver1, SRTM ver4. 1 and GEODATA DEM-9S ver3 digital ele-  
 463 vation models over Australia, *Australian Journal of Earth Sciences*, 57, 337–347, 2010.
- 464 Jing, C., Shortridge, A., Lin, S., and Wu, J.: Comparison and validation of SRTM and  
 465 ASTER GDEM for a subtropical landscape in Southeastern China, *International Journal*  
 466 *of Digital Earth*, 7, 969–992, 2014.
- 467 Khan, S., Hong, Y., Wang, J., Yilmaz, K., Gourley, J., Adler, R., Brakenridge, G., Policelli,  
 468 F., Habib, S., and Irwin, D.: Satellite remote sensing and hydrologic modeling for flood  
 469 inundation mapping in Lake Victoria basin: Implications for hydrologic prediction in  
 470 ungauged basins, *IEEE Transactions on Geoscience and Remote Sensing*, 49, 85–95, 2011.
- 471 Krupka, M., Pender, G., Wallis, S., Sayers, P., and Mulet-Marti, J.: A rapid flood inundation  
 472 model, in: *Proceedings of the Congress-International Association for Hydraulic Research*,  
 473 vol. 32, p. 28, 2007.



- 474 Lehner, B., Verdin, K., and Jarvis, A.: HydroSHEDS technical documentation, version 1.0,  
475 World Wildlife Fund US, Washington, DC, pp. 1–27, 2006.
- 476 Lehner, B., Verdin, K., and Jarvis, A.: New global hydrography derived from spaceborne  
477 elevation data, *Eos, Transactions American Geophysical Union*, 89, 93–94, 2008.
- 478 Lehner, B., Verdin, K., and Jarvis, A.: HydroSHEDS Technical Documentation Version 1.2,  
479 EOS Transactions, 2013.
- 480 Leopold, L.: *A View of the River*, Harvard University Press, 1994.
- 481 Lighthill, M. and Whitham, G.: On Kinematic Waves. I. Flood Movement in Long Rivers,  
482 *Proceedings of the Royal Society A: Mathematical, Physical and Engineering Sciences*,  
483 doi:10.1098/rspa.1955.0088, 1955.
- 484 Maione, U., Mignosa, P., and Tomirotti, M.: Regional estimation model of synthetic design  
485 hydrographs, *International Journal of River Basin Management*, 12, 151–163, 2003.
- 486 Merz, R. and Blöschl, G.: Flood frequency regionalisation? spatial proximity vs. catchment  
487 attributes, *Journal of Hydrology*, 302, 283–306, 2005.
- 488 Moel, H. d., Alphen, J. v., Aerts, J., et al.: Flood maps in Europe—methods, availability and  
489 use, *Nat. Hazards Earth Syst. Sci.*, 9, 2009.
- 490 Montanari, A.: Hydrology of the Po River: looking for changing patterns in river discharge,  
491 *Hydrology and Earth System Sciences*, 16, 3739–3747, 2012.
- 492 Neal, J., Schumann, G., and Bates, P.: A subgrid channel model for simulating river hy-  
493 draulics and floodplain inundation over large and data sparse areas, *Water Resources*  
494 *Research*, 48, 2012.
- 495 NERC, N. E. R. C. G. B.: *Flood Studies Report in Five Volumes*, NERC, 1975.
- 496 Pappenberger, F., Dutra, E., Wetterhall, F., and Cloke, H.: Deriving global flood hazard  
497 maps of fluvial floods through a physical model cascade, *Hydrology and Earth System*  
498 *Sciences*, 16, 4143–4156, 2012.
- 499 Paprotny, D., Morales-Nápoles, O., and Jonkman, S.: Efficient pan-European river flood haz-  
500 ard modelling through a combination of statistical and physical models, *Natural Hazards*  
501 *and Earth System Sciences*, 17, 1267, 2017.
- 502 Rabus, B., Eineder, M., Roth, A., and Bamler, R.: The shuttle radar topography mission—a  
503 new class of digital elevation models acquired by spaceborne radar, *ISPRS journal of*  
504 *photogrammetry and remote sensing*, 57, 241–262, 2003.
- 505 Rojas, R., Feyen, L., Dosio, A., and Bavera, D.: Improving pan-European hydrological  
506 simulation of extreme events through statistical bias correction of RCM-driven climate  
507 simulations., *Hydrology & Earth System Sciences*, 15, 2011.



- 508 Rudari, R., Silvestro, F., Campo, L., Rebora, N., Boni, G., and Herold, C.: Improvement  
509 of the Global Food Model for the GAR 2015, United Nations Office for Disaster Risk  
510 Reduction (UNISDR), Centro Internazionale in Monitoraggio Ambientale (CIMA), UNEP  
511 GRID-Arendal (GRID-Arendal): Geneva, Switzerland, p. 69, 2015.
- 512 Sampson, C., Smith, A., Bates, P., Neal, J., Alfieri, L., and Freer, J.: A high-resolution  
513 global flood hazard model, *Water resources research*, 51, 7358–7381, 2015.
- 514 Samuels, P.: Cross section location in one-dimensional models, in: *International Conference*  
515 *on River Flood Hydraulics*, Wiley, Chichester, pp. 339–350, 1990.
- 516 Te Linde, A., Aerts, J., and van den Hurk, B.: Effects of flood control measures and climate  
517 change in the Rhine basin, in: *Proceedings of the 4th International Symposium on Flood*  
518 *Defence*, Toronto, Canada, pp. 6–5, 2008.
- 519 Te Linde, A., Bubeck, P., Dekkers, J., De Moel, H., and Aerts, J.: Future flood risk estimates  
520 along the river Rhine, *Natural Hazards and Earth System Sciences*, 11, 459, 2011.
- 521 Tomassetti, B., Coppola, E., Verdecchia, M., and Visconti, G.: Coupling a distributed  
522 grid based hydrological model and MM5 meteorological model for flooding alert mapping,  
523 *Advances in Geosciences*, doi:10.5194/adgeo-2-59-2005, 2005a.
- 524 Tomassetti, B., Coppola, E., Verdecchia, M., and Visconti, G.: Coupling a distributed  
525 grid based hydrological model and MM5 meteorological model for flooding alert mapping,  
526 *Advances in Geosciences*, 2, 59–63, 2005b.
- 527 Verdecchia, M., Coppola, E., Faccani, C., Ferretti, R., Memmo, A., Montopoli, M., Rivolta,  
528 G., Paolucci, T., Picciotti, E., Santacasa, A., Tomassetti, B., Visconti, G., and Marzano,  
529 F.: Flood forecast in complex orography coupling distributed hydro-meteorological models  
530 and in-situ and remote sensing data, *Meteorology and Atmospheric Physics*, doi:10.1007/  
531 s00703-007-0278-z, 2008.
- 532 Verdecchia, M., Coppola, E., Tomassetti, B., and Visconti, G.: Cetemps Hydrological Model  
533 (CHyM), a Distributed Grid-Based Model Assimilating Different Rainfall Data Sources,  
534 in: *Hydrological Modelling and the Water Cycle*, pp. 165–201, Springer, 2009.
- 535 Winsemius, H., Aerts, J., van Beek, L., Bierkens, M., Bouwman, A., Jongman, B., Kwadijk,  
536 J., Ligtoet, W., Lucas, P., Van Vuuren, D., et al.: Global drivers of future river flood  
537 risk, *Nature Climate Change*, 6, 381, 2016.
- 538 Wolfram, S.: Cellular automata as models of complexity, *Nature*, 311, 419–424, 1984.
- 539 Wood, E., Roundy, J., Troy, T., Van Beek, L., Bierkens, M., Blyth, E., de Roo, A., Döll,  
540 P., Ek, M., Famiglietti, J., et al.: Hyperresolution global land surface modeling: Meeting  
541 a grand challenge for monitoring Earth’s terrestrial water, *Water Resources Research*, 47,  
542 2011.
- 543 Yamazaki, D., O’Loughlin, F., Trigg, M. A., Miller, Z. F., Pavelsky, T. M., and Bates, P. D.:



- 544 Development of the global width database for large rivers, *Water Resources Research*, 50,  
545 3467–3480, 2014.
- 546 Zhao, D., Shen, H., Tabios III, G., Lai, J., and Tan, W.: Finite-volume two-dimensional  
547 unsteady-flow model for river basins, *Journal of Hydraulic Engineering*, 120, 863–883,  
548 1994.